

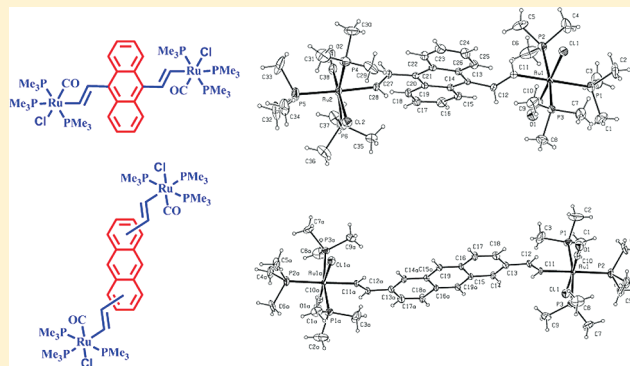
Synthesis, Characterization, and Properties of Anthracene-Bridged Bimetallic Ruthenium Vinyl Complexes $[\text{RuCl}(\text{CO})(\text{PMe}_3)_3]_2(\mu\text{-CH}=\text{CH}\text{-anthracene}\text{-CH}=\text{CH})$

Ya-Ping Ou, Chuanyin Jiang, Di Wu, Jianlong Xia, Jun Yin,* Shan Jin, Guang-Ao Yu, and Sheng Hua Liu*

Key Laboratory of Pesticide and Chemical Biology, Ministry of Education, College of Chemistry, Central China Normal University, Wuhan 430079, People's Republic of China

Supporting Information

ABSTRACT: Four anthracene-based bimetallic ruthenium vinyl complexes, in which two ruthenium units are attached at different positions (the 9,10-, 1,5-, 2,6-, and 1,8-positions) of the anthracene moiety, have been synthesized by treating the appropriate anthracene-based ethynes with $[\text{RuHCl}(\text{CO})(\text{PPh}_3)_3]$. These bimetallic complexes have been thoroughly characterized by NMR, X-ray diffraction, and elemental analysis. According to the single-crystal X-ray structures, the 2,6-disubstituted ruthenium vinyl complex has a more planar structure compared with the 9,10-disubstituted complex, possibly because it has less steric hindrance. Furthermore, we have investigated the optical electronic properties of these complexes, such as their UV/vis absorption spectra, fluorescence spectra, and electrochemical properties. The optical electronic results indicated that the 2,6-disubstituted ruthenium vinyl complex displayed the strongest fluorescence emission due to the more planar structure of its organic conjugated bridge, and the electrochemical studies showed that the two ruthenium centers displayed obvious differences in electronic communication when they are located at different positions on the anthracene unit, with the 9,10- and 1,8-disubstituted ruthenium vinyl complexes exhibiting better electronic communication and higher stability of the mixed-valence complex than the 1,5- and 2,6-disubstituted complexes.



INTRODUCTION

Molecular wires provide the theoretical and technological foundations of molecular electronic devices and have been widely applied in the development of molecular-level electronic computers.¹ Molecular wires based on conjugated organic molecules have attracted increasing attention as a result of their easy functionalization, convenient controllability, and low cost of organic molecules. Usually, the conjugated organic molecules have been directly linked to electrode surfaces as the simplest method for evaluating electron transfer, although this is inconvenient to perform on a large scale.² Therefore, as models of molecular wires, linear conjugated organic molecules with two redox-active organometallic termini, in which two metal atoms are linked by a conjugated organic bridge ligand, can be advantageously applied in investigations of electron transfer by electrochemical methods.³ Consequently, there have been many studies on conjugated organometallic molecular wires in recent years. The electronic interaction between the two redox-active metal centers mainly depends on the conjugated organic bridge ligand.⁴ Previous research in this area has mainly focused on linear conjugated metal complexes with sp - and sp^2 -hybridized organic bridges, such as oligoethynyl⁵ and oligovinyl-bridged⁶ metal complexes.

Polycyclic aromatic hydrocarbons (PAHs), as classical conjugated systems, have been widely applied in organic semiconductor materials, such as organic light-emitting diodes (OLEDs), field-effect transistors (FETs), and solar cells.⁷ Acenes, as the simplest PAHs, have been widely used as optical electronic materials for electronic devices, due to their simple synthesis and easy functionalization.⁸ In the field of organometallic molecular wires, acenes have been applied as organic bridging units, and their mediation of electron transfer has been investigated. For example, some research groups have reported naphthylene- and anthracene-based bimetallic complexes and have studied their electron-transfer properties.⁹ Recently, Yip also described tetracene-based bimetallic complexes.¹⁰ However, from a survey of the literature, we noted that the metal atoms were often introduced at the active sites of the acene, such as the 1,4-positions of naphthylene, the 9,10-positions of anthracene, and the 5,12-positions of tetracene, presumably because of the ease of synthesis. In contrast, the introduction of metal atoms at the terminal positions of the acene, such as the 1,5-, 2,6-, and 1,8-positions of anthracene, is synthetically challenging. Recently,

Received: July 11, 2011

Published: October 11, 2011

Abruña reported a series of bipyridine ruthenium complexes differently substituted at the 1,5-, 2,6-, and 2,7-positions.^{9b} In our recent work, we reported a series of anthracene quinone based bimetallic ruthenium vinyl complexes (Scheme 1), in which the ruthenium atoms were attached at the 1,4-, 1,5-, 2,6-, and 1,8-positions of the anthracene quinone.¹¹ The electrochemical properties of these complexes showed that the interaction between the two metal centers was not very obvious. This research inspired us to explore the properties of 9,10-, 1,5-, 2,6-, and 1,8-disubstituted anthracene bimetallic ruthenium vinyl complexes. In the work described herein, we have designed and synthesized four bimetallic ruthenium vinyl complexes incorporating anthracene units (Scheme 2), in which the ruthenium atoms were introduced at the 9,10-, 1,5-, 2,6-, and 1,8-positions of anthracene through vinyl bridges. These bimetallic complexes have been thoroughly characterized by NMR, X-ray diffraction, and elemental analysis. Furthermore, we have investigated their UV/vis absorption and fluorescence spectra, as well as their electrochemical properties. Their optical electronic properties indicated that the 2,6-disubstituted ruthenium vinyl complex displayed the strongest fluorescent emission, while the electrochemical studies showed that two ruthenium centers located at different positions on the anthracene unit had markedly different degrees of electronic communication, with the 9,10- and 1,8-disubstituted ruthenium vinyl complexes exhibiting better electronic communication and greater stability of the mixed-valence system than the 1,5- and 2,6-disubstituted complexes.

RESULTS AND DISCUSSION

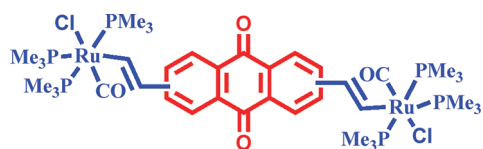
Syntheses and Characterization. The general synthetic route for the preparation of anthracene-based bimetal ruthenium vinyl complexes **1a–d** is outlined in Scheme 3. The regioisomeric anthracene bromides or iodides **2a–d** were selected as starting materials to perform Sonogashira coupling reactions with (trimethylsilyl)acetylene in the presence of a Pd/Cu

catalyst. The respective bis[(trimethylsilyl)ethynyl]anthracenes **3a–d** were obtained in yields of 47–85%. After the TMS groups were removed in methanolic KOH solution, the bis(ethynyl)anthracenes **4a–d** were obtained in yields of 39–86%. The bis(ethynyl)anthracenes **4a–d** were then reacted with the ruthenium hydride complex $[\text{RuHCl}(\text{CO})(\text{PPh}_3)_3]$ to give the insertion products $[(\text{PPh}_3)_2\text{Cl}(\text{CO})\text{Ru}]_2(\mu\text{-CH}=\text{CH}\text{-ant-CH}=\text{CH})$, which were not isolated because these five-coordinated complexes are air-sensitive, especially in solution. Thus, PMe_3 was added directly to give the corresponding six-coordinated complexes **1a–d**. These complexes were characterized by ^1H , ^{13}C , and ^{31}P NMR. Although complexes **1a–d** have similar structures, the resonance signals such as those of the $\text{CH}=\text{CH}$ protons in the ^1H NMR spectra and of PMe_3 in the ^{31}P NMR spectra displayed obvious differences, which can be attributed to the differences in substitution positions on the anthracene moiety. Fortunately, we were able to obtain single-crystal X-ray structures of the 9,10- and 2,6-disubstituted anthracene bimetallic ruthenium vinyl complexes **1a,c**.

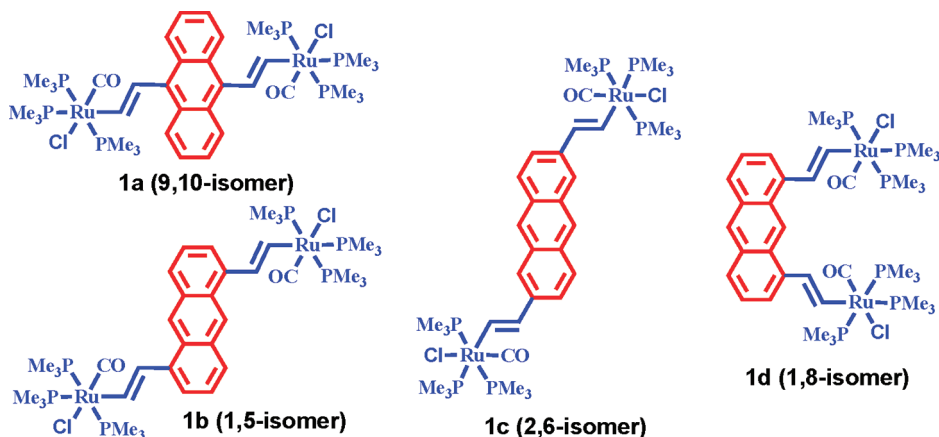
X-ray Structures of 1a,c. Single crystals of complexes **1a,c** suitable for X-ray analysis were obtained by slow diffusion of hexane into solutions in dichloromethane and chloroform, respectively. The single-crystal X-ray structures of complexes **1a,c** are depicted in Figures 1 and 2, respectively. The crystallographic details are given in Table 1. Selected bond distances and angles for **1a,c** are presented in Tables 2 and 3, respectively. According to the crystal structure of complex **1a** in Figure 1A, its C11–C12 and C27–C28 bond lengths are 1.335 and 1.318 Å, respectively. These bond lengths lie between those of carbon–carbon single and triple bonds, indicating that they correspond to carbon–carbon double bonds. Furthermore, we found these carbon–carbon double bonds to be in a trans configuration. As shown in Figure 1, two carbon–carbon double bonds are not coplanar with the anthracene moiety, possibly because of steric hindrance. The two dihedral angles between the planes defined by C11–C12–C13 and C28–C27–C20 with respect to the central benzene ring of the anthracene moiety are 40.76 and 66.80°, respectively, further confirming that the anthracene and vinyl units are not coplanar, as shown in Figure 1B.

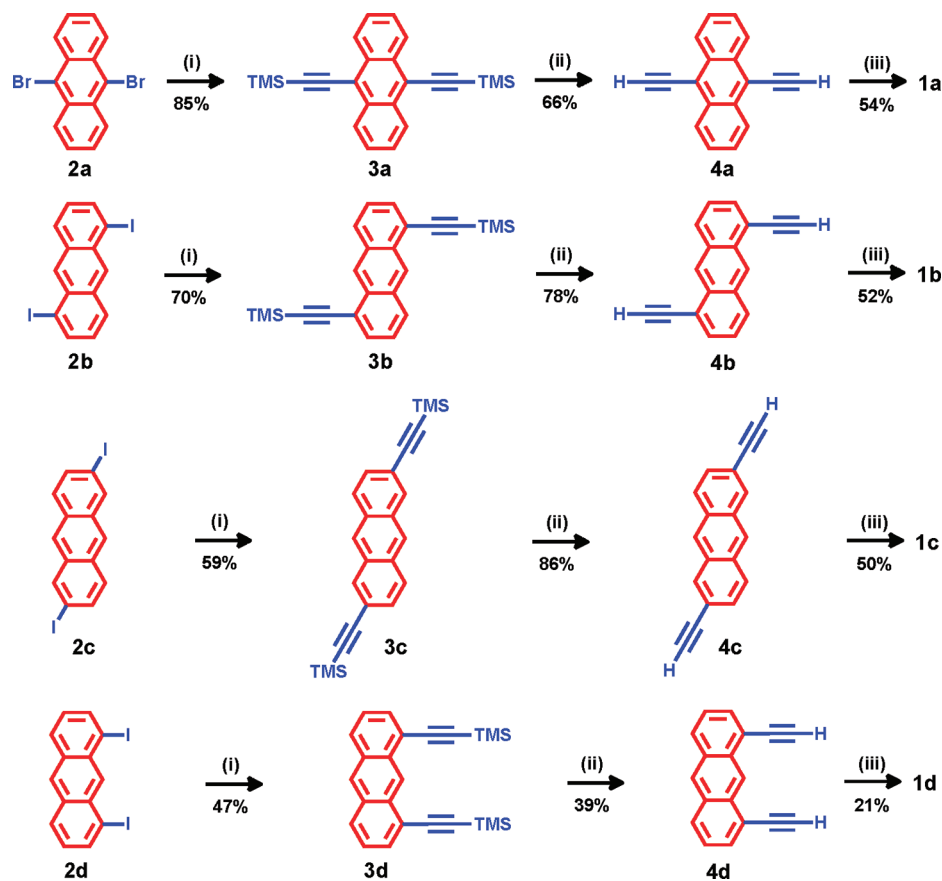
In Figure 2, the C11–C12 and C11a–C12a bond lengths in complex **1c** are both seen to be 1.318 Å, indicating that they correspond to carbon–carbon double bonds and are in a trans configuration. At the same time, the Ru1–Ru1a distance in complex **1c** is 15.924 Å, which is longer than that in complex **1a**

Scheme 1. Anthraquinone-Based Binuclear Ruthenium Vinyl Complexes



Scheme 2. Anthracene-Based Binuclear Ruthenium Vinyl Complexes 1a–d



Scheme 3^a

^a Reaction reagents and conditions: (i) TMSA, Pd(PPh₃)₄, CuI, toluene or THF/Et₃N; (ii) KOH, THF/MeOH; (iii) RuHCl(CO)(PPh₃)₃, PMe₃, CH₂Cl₂.

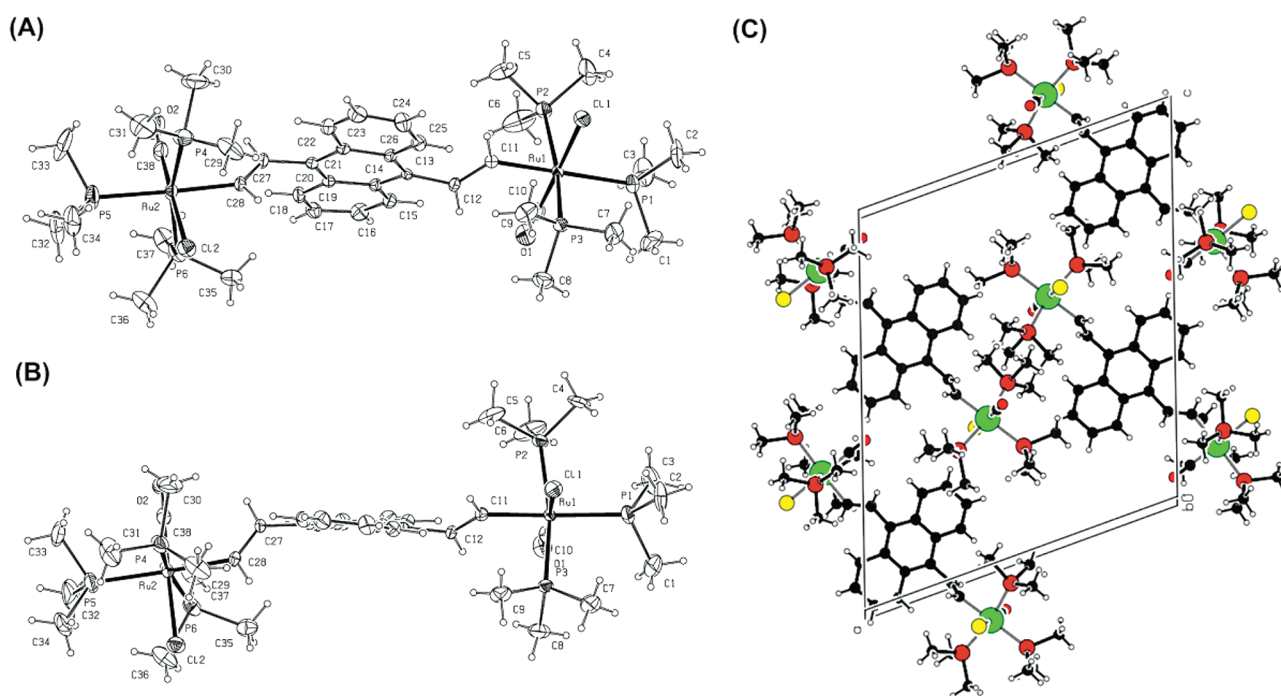


Figure 1. Single-crystal structure of complex 1a: (A) top view; (B) side view; (C) packing view.

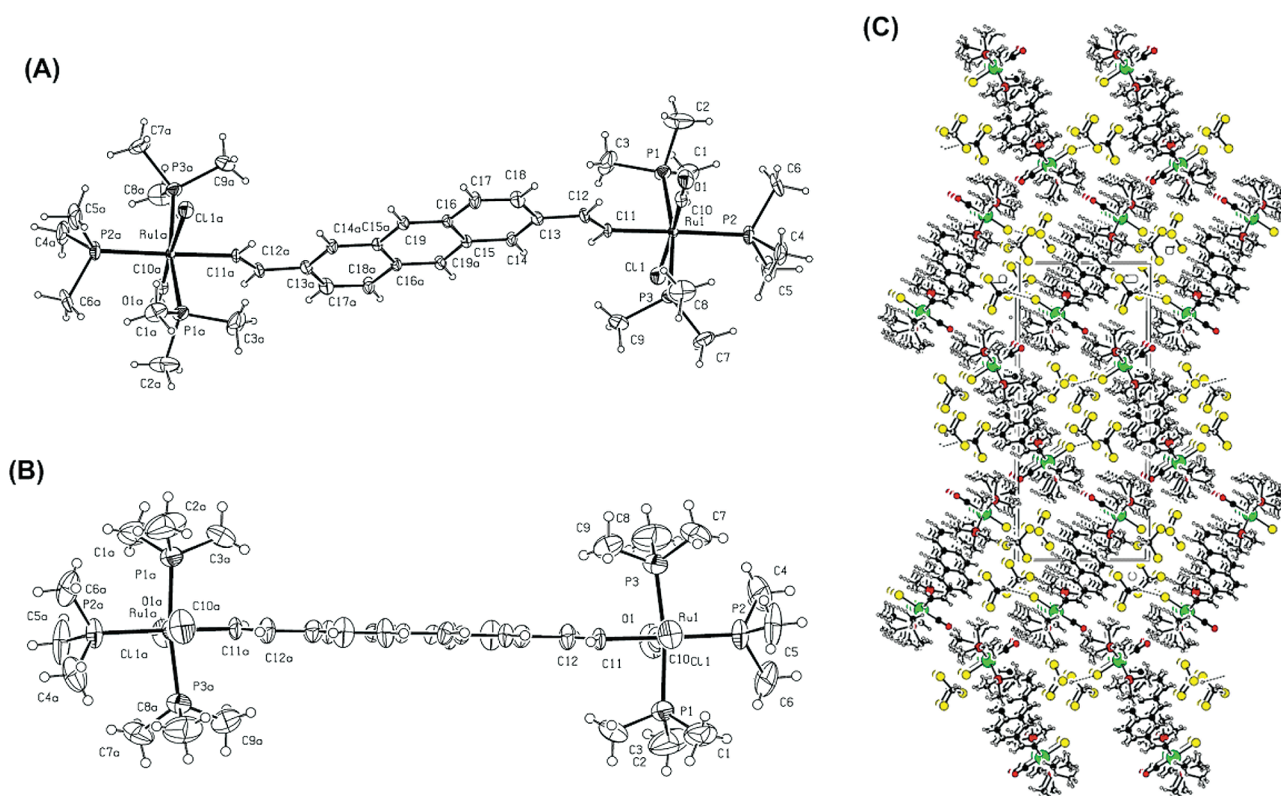


Figure 2. Single-crystal structure of complex **1c**: (A) top view; (B) side view; (C) packing view.

(11.847 Å). According to Figure 2A, complex **1c** has a very symmetrical structure. Furthermore, in comparison with our reported single-crystal structure of $[\{\text{Ru}(\text{PMe}_3)_2(\text{CO})\text{Cl}\}_2(\mu\text{-CH}=\text{CH}\text{-Aq}\text{-CH}=\text{CH}\text{-1,5})]$ (Aq = anthraquinone),¹¹ the core ligand anthracene has a planar rigid structure; the anthracene and vinyl units are also coplanar in Figure 2B. Such coplanarity of the anthracene and vinyl units is favorable for forming strong $\pi\text{-}\pi$ interactions between molecules.

UV/vis Absorption and Fluorescence Spectra. Figure 3A shows the UV/vis absorption spectra of complexes **1a–d** in CH_2Cl_2 at room temperature. According to the data in Table 4, the 9,10-, 1,5-, and 1,8-disubstituted ruthenium vinyl complexes **1a,b,d** exhibited three very similar absorption bands. However, the 2,6-disubstituted ruthenium vinyl complex **1c** showed a completely different UV/vis absorption spectrum. For example, complexes **1a,b,d** showed a rather intense electronic transition at about 275 nm, while the intense electronic transition of complex **1c** appeared at 327 nm. Moreover, the absorption maxima of complex **1c** showed obvious red shifts, which indicated that the 2,6-disubstituted complex **1c** had more extensive conjugation. In addition, the other broad absorption bands of complexes **1a–d** at 400–500 nm can be attributed to MLCT (metal-to-ligand charge transfer), which is similar to that for bimetal complexes of anthraquinone-based bridging ligands.¹¹

Subsequently, the fluorescence properties of complexes **1a–d** were investigated in dichloromethane solution (2×10^{-5} mol/L) at room temperature. From the fluorescence properties of complexes **1a–d** shown in Figure 3B, it can be seen that the complexes **1a,b,d** displayed very weak fluorescence. In comparison with complexes **1a,b,d**, the 2,6-disubstituted ruthenium vinyl complex **1c** showed very strong fluorescence properties and the highest fluorescence quantum yield, presumably as a

result of its greater conjugation and the coplanarity of the organic bridge. In general, increasing the molecular rigidity and coplanarity will increase the fluorescence intensity and improve the fluorescence quantum yield, which is possibly attributed to an increase in π -electronic conjugation. Furthermore, the coplanarity of the conjugated anthracene-based vinyl bridge was favorable for molecular packing, which was in good agreement with the single-crystal X-ray structure. In Figure 2C, the packing view of the 2,6-disubstituted ruthenium vinyl complex shows a highly ordered intermolecular interaction, while no such interaction is observed in the packing view of the 9,10-disubstituted ruthenium vinyl complex **1a**, as shown in Figure 1C.

The PL efficiency (Φ_{PL}) of complexes **1a–d** in CH_2Cl_2 solutions was measured by using quinine sulfate (ca. 1×10^{-5} M solution in 0.1 M H_2SO_4 , assuming Φ_{PL} of 0.55) as a standard.

Electrochemical Properties. The interaction between the two metal centers linked via an anthracene-based vinyl bridge was examined by electrochemical methods. Cyclic voltammetry (CV) and square-wave voltammetry (SWV) were used to study the electrochemical behavior of complexes **1a–d** (in 0.1 M Bu_4NPF_6 in CH_2Cl_2). Cyclic and square-wave voltammograms (CVs and SWVs) for complexes **1a–d** are depicted in Figure 4. As shown in Figure 4A, all of the complexes underwent two successive single-electron oxidation processes in CH_2Cl_2 and exhibited two pairs of independent single-electron oxidation waves, corresponding to oxidation of $\text{Ru}^{\text{II,II}}$ to $\text{Ru}^{\text{II,III}}$ and then of $\text{Ru}^{\text{II,III}}$ to $\text{Ru}^{\text{III,III}}$, respectively. For complex **1a**, the potential difference ΔE was 393 mV with a corresponding K_c value of 4.57×10^6 when the two ruthenium terminal groups were attached at the active 9,10-positions of anthracene, which indicated that electron density can be easily transferred from one ruthenium center to the other. Furthermore, in comparison

Table 1. Crystal Data and Data Collection and Refinement Parameters for 1a,c^a

	complex 1a	complex 1c
formula	C ₃₈ H ₆₈ Cl ₂ O ₂ P ₆ Ru ₂	C ₄₂ H ₇₀ Cl ₁₄ O ₂ P ₆ Ru ₂
fw	1013.77	1491.24
temp (K)	298(2)	298(2)
cryst syst	monoclinic	monoclinic
space group	P2 ₁ /c	P2 ₁ /n
a (Å)	17.5343(11)	10.3117(19)
b (Å)	13.9458(9)	12.025(2)
c (Å)	21.0762(13)	27.538(5)
α (deg)	90.00	90.00
β (deg)	109.0590(10)	97.221(4)
γ (deg)	90.00	90.00
V (Å ⁻³)	4871.2(5)	3387.5(11)
Z	4	2
D _{calcd} (g cm ⁻³)	1.382	1.462
F(000)	2088	1508
cryst size (mm)	0.16 × 0.12 × 0.10	0.16 × 0.12 × 0.10
radiation, Mo Kα (Å)	0.710 73	0.710 73
abs coeff (mm ⁻¹)	0.956	1.170
θ range (deg)	1.78–25.50	1.85 to 25.01
total no. of rflns	48 568	19 848
no. of indep rflns	9057 (0.1216)	5969 (0.0671)
no. of data/restraints/params	9057/0/469	5969/0/307
final R	0.0732	0.0873
R _w	0.1333	0.1818
R (all data)	0.1315	0.1098
R _w (all data)	0.1512	0.1917
goodness of fit/F ²	1.036	1.182
largest diff peak, hole (e Å ⁻³)	1.337, -0.772	0.871, -1.154

^a $w = 1/[\sigma^2(F_o)^2 + (aP)^2 + bP]$, where $P = (F_o^2 + F_c^2)/3$.

Table 2. Selected Bond Lengths (Å) and Angles (deg) for 1a

bond length (Å)		bond angle (deg)	
C(11)–C(12)	1.335(8)	C(11)–C(12)–C(13)	130.9(6)
C(12)–C(13)	1.486(8)	C(28)–C(27)–C(20)	125.8(6)
C(20)–C(27)	1.489(8)	C(12)–C(11)–Ru(1)	130.8(5)
C(27)–C(28)	1.319(8)	C(11)–Ru(1)–P(1)	176.60(19)
Ru(1)–C(10)	1.839(9)	C(11)–Ru(1)–P(2)	82.74(18)
Ru(2)–C(28)	2.109(6)	C(11)–Ru(1)–P(3)	86.39(18)

with the 9,10-disubstituted anthracene-based ethynyl bimetallic ruthenium complexes, the bimetallic ruthenium vinyl complex **1a** performed better.⁹ At the same time, the more extensive π system of complex **1a** led to better electronic interaction between the ruthenium centers than we have reported for [RuCl(CO)-(PMe₃)₃]₂(μ -CH=CH-Ar-CH=CH) with 4,4'-diethynylphenyl as the spacer ($\Delta E = 296$ mV, $K_c = 1.04 \times 10^5$).¹² However, when the ruthenium subunits were attached to the two terminal rings of the anthracene unit, the 1,5- and 2,6-disubstituted complexes **1b,c** showed lower potential differences ΔE (250 mV for complex **1b** and 224 mV for complex **1c**), while the data for the 1,8-disubstituted ruthenium complex **1d** confirmed that

Table 3. Selected Bond Lengths (Å) and Angles (deg) for 1c

bond length (Å)		bond angle (deg)	
C(11)–C(12)	1.318(10)	C(11)–C(12)–C(13)	126.6(7)
C(12)–C(13)	1.495(10)	C(14)–C(15)–C(16)	118.8(6)
C(13)–C(14)	1.369(10)	C(12)–C(11)–Ru(1)	132.1(6)
C(14)–C(15)	1.430(9)	C(11)–Ru(1)–P(1)	86.5(2)
C(16)–C(19)	1.390(10)	C(11)–Ru(1)–P(2)	178.8(2)
Ru(1)–C(11)	2.085(6)	C(11)–Ru(1)–P(3)	84.0(2)

this bimetallic ruthenium complex displayed better electron transfer, with a potential difference ΔE of 396 mV, as shown in Table 5. According to the electrochemical data for complexes **1a–d**, we found that the different positions of attachment of the two ruthenium centers on the anthracene affects electronic communication, with the 9,10- and 1,8-disubstituted ruthenium vinyl complexes displaying stronger metal–metal electron transfer and greater stability of the mixed-valence system than the 1,5- and 2,6-disubstituted complexes, possibly due to the lengths of the conjugation pathways between the ruthenium centers. In addition, from electrochemical properties of two bimetal complexes containing different core ligands, we find the following: (1) anthraquinone-based 1,5-Aq-diRu, 2,6-Aq-diRu, 1,8-Aq-diRu, $\Delta E = 75$ mV, 2,6-Aq-diRu has no clear sign of peak separation, 100 mV, respectively; (2) anthracene-based 1,5-Ant-diRu, 2,6-Ant-diRu, 1,8-Ant-diRu, $\Delta E = 250, 224, 396$ mV, respectively. We also found that these anthracene-based ruthenium vinyl complexes had better electronic communication in comparison with the anthracene quinone based ruthenium vinyl complexes described in our previous report.¹¹ This can be attributed to two reasons: one is that the electron-withdrawing carbonyl decreases the electronic interaction between the two metal centers and the other is that, according to the crystal structures of two series of bimetal complexes, the rigidity and coplanarity of the anthracene bridging ligand are stronger than those of the anthraquinone bridging ligand and lead to increasing interaction between the two metal centers.

In conclusion, we have designed and synthesized four bimetallic ruthenium vinyl complexes containing an anthracene unit, to which ruthenium subunits were attached at the 9,10-, 1,5-, 2,6-, and 1,8-positions through vinyl bridges. The UV/vis absorption spectra, fluorescence spectra, and electrochemical properties of the complexes have been studied in detail. Their optical electronic properties indicated that the 2,6-disubstituted ruthenium vinyl complex displayed the strongest fluorescence emission because of highly ordered intermolecular interactions. The electrochemical studies showed that different locations of the two ruthenium centers on the anthracene unit led to obvious differences in electronic communication, with the 9,10- and 1,8-disubstituted ruthenium vinyl complexes exhibiting better electronic communication and higher stability of the mixed-valence system than the 1,5- and 2,6-disubstituted complexes, possibly due to the lengths of the conjugation pathways between the ruthenium centers. Therefore, our studies highlight an interesting difference in the properties of regioisomerically substituted acenes. In this specific case, our research forms the basis for designing and constructing larger π -system architectures as organic bridges in organometallic molecular wires and should be helpful in understanding the electron transfer between different sites.

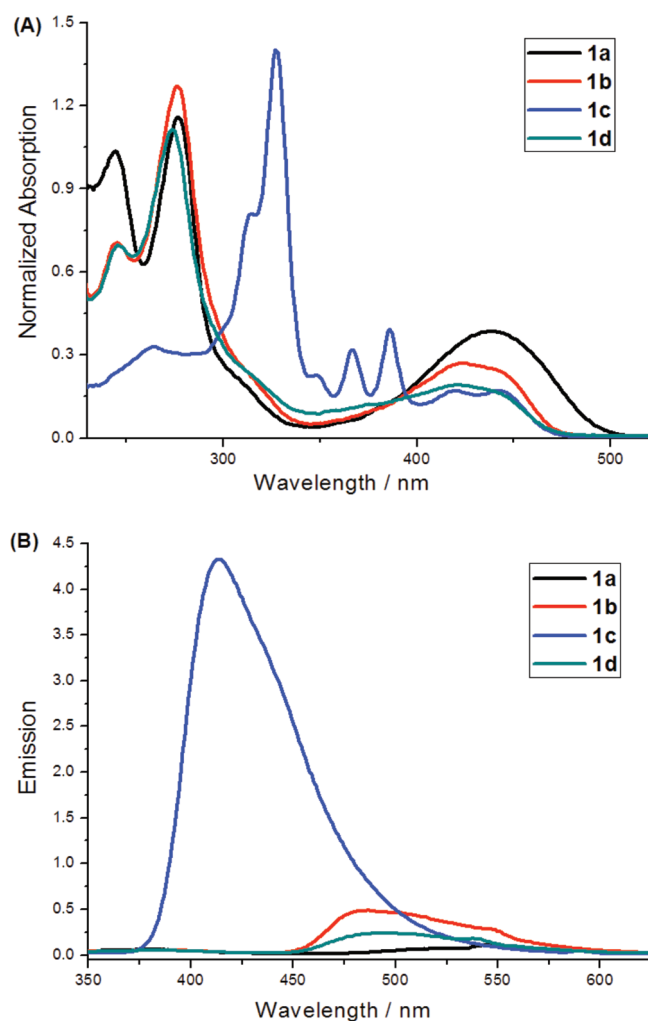


Figure 3. (A) UV-vis absorption spectrum of compounds **1a–d** in CH_2Cl_2 . (B) Fluorescence spectra of compounds **1a–d** (2×10^{-5} mol/L) in CH_2Cl_2 .

Table 4. Absorption Characteristics and Fluorescence Quantum Yields of Complexes **1a–d** in CH_2Cl_2 (2×10^{-5} mol/L)

complex	absorption λ_{max} (nm)/ $10^{-4}\epsilon_{\text{max}}$ ($\text{cm}^{-1}\text{M}^{-1}$)	emission λ_{max} (nm)	$10^2\Phi_{\text{PL}}$
1a	244 (5.18), 276 (5.80), 437 (1.94)	545	0.062
1b	245 (3.53), 276 (6.37), 423 (1.35)	486	0.236
1c	264 (1.65), 314 (4.06), 327 (7.02), 348 (1.15), 366 (1.59), 386 (1.97), 420 (0.85), 442 (0.86)	475	0.897
1d	245 (3.49), 274 (5.57), 421 (0.97)	494	0.153

EXPERIMENTAL SECTION

General Materials. All manipulations were carried out at room temperature under a nitrogen atmosphere using standard Schlenk techniques, unless otherwise stated. Solvents were predried, distilled, and degassed prior to use, except those for spectroscopic measurements, which were of spectroscopic grade. The reagent 9,10-dibromoanthracene (**2a**) was commercially available. The starting materials $\text{RuHCl}(\text{CO})(\text{PPh}_3)_3$,

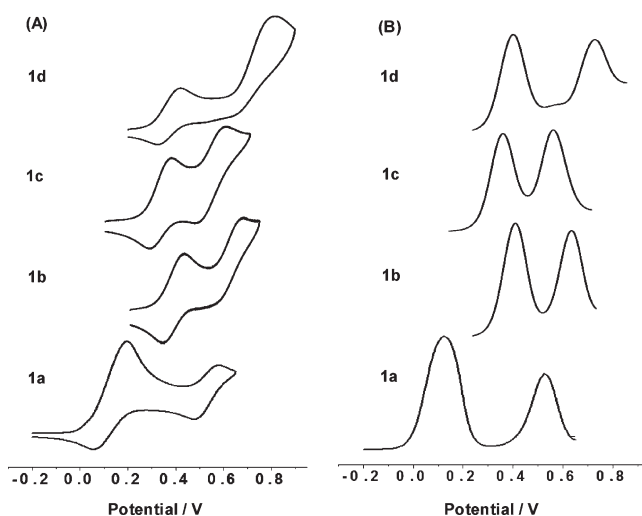


Figure 4. (A) Cyclic voltammograms (CV) of complexes **1a–d** in $\text{CH}_2\text{Cl}_2/\text{Bu}_4\text{NPF}_6$ at $\nu = 0.1 \text{ V s}^{-1}$ and (B) square-wave voltammograms (SWV) of complexes **1a–d** at $f = 10 \text{ Hz}$.

Table 5. Electrochemical Data for Complexes **1a–d**

complex	E_p^1 (V) ^a	$i_{p,a}/i_{p,c}$ ^b	E_p^2 (V) ^c	ΔE (mV) ^b	K_c ^d
1a	0.197	0.45	0.580	393	4.57×10^6
1b	0.430	0.62	0.680	250	1.73×10^4
1c	0.374	0.46	0.598	224	6.27×10^3
1d	0.420	0.52	0.816	396	5.15×10^6

^a From cyclic or square-wave voltammetry in 0.1 M $\text{CH}_2\text{Cl}_2/n\text{-Bu}_4\text{NPF}_6$ solutions at a scan rate of 100 mV/s for CV and 10 Hz for SWV. ^b Anodic/cathodic peak current ratios. ^c Peak potential differences $\Delta E = E_p^2 - E_p^1$. ^d The comproportionation constants, K_c , were calculated by the formula $K_c = \exp(\Delta E_{1/2}/25.69)$ at 298 K.

1,5-diidoanthracene (**2b**),¹⁴ 2,6-diidoanthracene (**2c**),^{15,16} and 1,8-diidoanthracene (**2d**)¹⁷ were prepared by the procedures described in the literature.

Synthesis of Bis((trimethylsilyl)ethynyl)anthracene. 9,10-Bis((trimethylsilyl)ethynyl)anthracene (**3a**).¹⁸ To a stirred solution of 9,10-dibromoanthracene (**2a**; 1.0 g, 3.9 mmol), CuI (0.07 g, 0.39 mmol), and $\text{Pd}(\text{PPh}_3)_4$ (0.45 g, 0.39 mmol) in triethylamine (60 mL) and THF (100 mL) under an argon atmosphere was added (trimethylsilyl)acetylene (0.95 g, 9.75 mmol), and the mixture at 60 °C was refluxed for 20 h. The cold solution was filtered through a bed of Celite. The filtrate was evaporated under reduced pressure and purified by silica gel column chromatography (petroleum ether) to give a red solid (0.91 g, 85%). ¹H NMR (400 MHz, CDCl_3): δ (ppm) 0.42 (s, 18H, SiCH_3), 7.60 (dd, $J = 3.6 \text{ Hz}$, 4H), 8.57 (dd, $J = 3.6 \text{ Hz}$, 4H).

1,5-Bis((trimethylsilyl)ethynyl)anthracene (**3b**).¹⁹ The procedure for **3b** was similar to that for **3a**: **2b** (1.0 g, 2.32 mmol), CuI (0.046 g, 0.24 mmol), $\text{Pd}(\text{PPh}_3)_4$ (0.28 g, 0.24 mmol), triethylamine (60 mL), THF (60 mL), (trimethylsilyl)acetylene (0.56 g, 5.8 mmol). Yield: 0.60 g (70%) of a light yellow solid. ¹H NMR (400 MHz, CDCl_3): δ (ppm) 0.39 (s, 18H, SiCH_3), 7.44 (t, $J = 6.8 \text{ Hz}$, 2H), 7.75 (d, $J = 6.8 \text{ Hz}$, 2H), 8.07 (d, $J = 8 \text{ Hz}$, 2H), 8.88 (s, 2H).

2,6-Bis((trimethylsilyl)ethynyl)anthracene (**3c**).¹⁹ The procedure for **3c** was similar to that for **3a**, with THF being replaced by toluene: **2c** (2.0 g, 4.65 mmol), CuI (0.09 g, 0.46 mmol), $\text{Pd}(\text{PPh}_3)_4$ (0.54 g, 0.46 mmol), triethylamine (60 mL), THF (100 mL), (trimethylsilyl)acetylene (0.56 g, 11.6 mmol). Yield: 1.02 g (59%) of a light yellow solid.

^1H NMR (400 MHz, CDCl_3): δ (ppm) 0.31 (s, 18H, SiMe_3), 7.46 (dd, $J = 7.2$ Hz, 2H), 7.91 (dd, $J = 8.8$ Hz, 2H), 8.14 (s, 2H), 8.30 (s, 2H).

1,8-Bis((trimethylsilyl)ethynyl)anthracene (3d).²⁰ The procedure of **3d** was similar to that for **3a**, with triethylamine being replaced by diisopropylamine: **2d** (1.5 g, 3.49 mmol), CuI (0.068 g, 0.35 mmol), Pd(PPh_3)₄ (0.41 g, 0.35 mmol), diisopropylamine (60 mL), THF (100 mL), (trimethylsilyl)acetylene (0.85 g, 8.7 mmol). Yield: 0.61 g (47%) of a yellow solid. ^1H NMR (400 MHz, CDCl_3): δ (ppm) 0.46 (s, 18H, SiMe_3), 7.49 (t, $J = 7.6$ Hz, 2H), 7.86 (d, $J = 6.8$ Hz, 2H), 8.04 (d, $J = 8.4$ Hz, 2H), 8.48 (s, 1H), 9.39 (s, 1H).

Synthesis of Diethynylanthracene. **9,10-Diethynylanthracene (4a).**²¹ **9,10-Bis((trimethylsilyl)ethynyl)anthracene (3a)**; 0.5 g, 1.35 mmol) was dissolved in a mixture of THF and methanol (30 mL, 1/1, v/v). Potassium hydroxide (0.16 g, 2.84 mmol) was added, and the reaction mixture was stirred at room temperature for 2 h. The reaction mixture was diluted with dichloromethane and washed with brine. The organic layer was dried over Na_2SO_4 and the solvent was removed in vacuo. The crude product was purified by chromatography (petroleum ether/dichloromethane 8/1). Yield: 0.2 g (66%) of a carmine solid. ^1H NMR (400 MHz, CDCl_3): δ (ppm) 4.07 (s, 2H, $\text{C}\equiv\text{CH}$), 7.61 (dd, $J = 3.6$ Hz, 4H), 8.60 (dd, $J = 3.6$ Hz, 4H).

1,5-Diethynylanthracene (4b).²² The procedure for **4b** was similar to that for **4a**: **3b** (0.33 g, 0.89 mmol), potassium hydroxide (0.12 g, 2.16 mmol), THF (20 mL), methanol (20 mL). The crude product was purified by chromatography (petroleum ether/dichloromethane 8/1). Yield: 0.16 g (78%) of a light yellow solid. ^1H NMR (400 MHz, CDCl_3): δ (ppm) 3.59 (s, 2H, $\text{C}\equiv\text{CH}$), 7.45 (t, $J = 7.2$ Hz, 2H), 7.78 (d, $J = 7.2$ Hz, 2H), 8.09 (d, $J = 8.8$ Hz, 2H), 8.93 (s, 2H).

2,6-Diethynylanthracene (4c).²² The procedure for **4c** was similar to that for **4a**: **3c** (0.21 g, 0.57 mmol), potassium hydroxide (0.08 g, 1.36 mmol), THF (30 mL), methanol (30 mL). The crude product was purified by chromatography (petroleum ether/dichloromethane 2/1). Yield: 0.11 g (86%) of a light yellow solid. ^1H NMR (400 MHz, CDCl_3): δ (ppm) 3.23 (s, 2H, $\text{C}\equiv\text{CH}$), 7.49 (dd, $J = 8.8$ Hz, 2H), 7.95 (dd, $J = 8.8$ Hz, 2H), 8.19 (s, 2H), 8.35 (s, 2H).

1,8-Diethynylanthracene (4d).²¹ The procedure for **4d** was similar to that for **4a**: **3d** (0.5 g, 1.35 mmol), flaky potassium hydroxide (0.18 g, 3.24 mmol), THF (20 mL), methanol (20 mL). The crude product was purified by chromatography (pure petroleum ether). Yield: 0.12 g (39%) of a yellow solid. ^1H NMR (400 MHz, CDCl_3): δ (ppm) 3.62 (s, 2H, $\text{C}\equiv\text{CH}$), 7.45 (t, $J = 7.6$ Hz, 2H), 7.79 (d, $J = 6.8$ Hz, 2H), 8.03 (d, $J = 8.4$ Hz, 2H), 8.45 (s, 1H), 9.44 (s, 1H).

General Synthesis of Binuclear Ruthenium Complexes¹¹

To a suspension of $\text{RuHCl}(\text{CO})(\text{PPh}_3)_3$ (0.42 g, 0.44 mmol) in CH_2Cl_2 (20 mL) was slowly added a solution of the corresponding diethynylanthracene (0.05 g, 0.22 mmol) in CH_2Cl_2 (5 mL). The reaction mixture was stirred for 30 min to give a red solution. Then a 1 M THF solution of PMe_3 (2.2 mL, 2.2 mmol) was added to the red solution. The mixture was stirred for another 20 h. The solution was reduced to ca. 2 mL under vacuum. Addition of hexane (30 mL) to the residue produced a yellow solid, which was collected by filtration, washed with hexane, and dried under vacuum.

$[\{\text{Ru}(\text{PMe}_3)_2(\text{CO})\text{Cl}\}_2(\mu\text{-CH}=\text{CH-ant-CH}=\text{CH-9,10})]$ (**1a**). Yield: 0.120 g, 54%. ^1H NMR (400 MHz, CDCl_3): δ (ppm) 1.52 (t, $J(\text{PH}) = 2.4$ Hz, 36H, PMe_3), 1.54 (d, $J(\text{PH}) = 3.2$ Hz, 18H, PMe_3), 7.31 (dd, $J(\text{HH}) = 3.6$ Hz, 4H), 7.52–7.58 (m, 2H, ant-CH=), 7.71–7.78 (m, 2H, Ru-CH=), 8.60 (dd, $J(\text{HH}) = 3.2$ Hz, 4H). ^{13}C NMR (100 MHz, CDCl_3): δ (ppm) 17.40 (t, $J = 14.9$ Hz, PMe_3), 20.04 (d, $J = 20.6$ Hz, PMe_3), 123.19, 127.11, 128.67, 133.14, 135.85 (ant-CH=), 170.80 (Ru-CH=), 202.41 (CO). ^{31}P NMR (160 MHz, CDCl_3): δ (ppm) –19.58 (t, $J = 22.56$ Hz, PMe_3), –7.80 (d, $J = 22.56$ Hz, PMe_3). Anal. Calcd for $\text{C}_{38}\text{H}_{66}\text{Cl}_2\text{O}_2\text{P}_6\text{Ru}_2$: C, 45.02; H, 6.56. Found: C, 45.15; H, 6.67.

$[\{\text{Ru}(\text{PMe}_3)_2(\text{CO})\text{Cl}\}_2(\mu\text{-CH}=\text{CH-ant-CH}=\text{CH-1,5})]$ (**1b**). Yield: 0.117 g, 52%. ^1H NMR (400 MHz, CDCl_3): δ (ppm) 1.46 (t, $J(\text{PH}) = 3.6$ Hz,

36H, PMe_3), 1.52 (d, $J(\text{PH}) = 6.8$ Hz, 18H, PMe_3), 7.39 (t, $J(\text{HH}) = 7.6$ Hz, 2H), 7.52–7.55 (m, 2H, ant-CH=), 7.56 (d, $J(\text{HH}) = 6.8$ Hz, 2H), 7.80 (d, $J(\text{HH}) = 8.4$ Hz, 2H), 8.26–8.33 (m, 2H, Ru-CH=), 8.34 (s, 2H). ^{13}C NMR (100 MHz, CDCl_3): δ (ppm) 16.88 (t, $J = 15.7$ Hz, PMe_3), 20.23 (d, $J = 20.6$ Hz, PMe_3), 120.18, 122.60, 123.25, 125.34, 128.95, 131.38, 132.11, 138.79 (ant-CH=), 169.91 (Ru-CH=), 202.52 (CO). ^{31}P NMR (160 MHz, CDCl_3): δ (ppm) –17.55 (t, $J = 22.6$ Hz, PMe_3), –5.68 (d, $J = 22.6$ Hz, PMe_3). Anal. Calcd for $\text{C}_{38}\text{H}_{66}\text{Cl}_2\text{O}_2\text{P}_6\text{Ru}_2$: C, 45.02; H, 6.56. Found: C, 45.19; H, 6.48.

$[\{\text{Ru}(\text{PMe}_3)_2(\text{CO})\text{Cl}\}_2(\mu\text{-CH}=\text{CH-ant-CH}=\text{CH-2,6})]$ (**1c**). Yield: 0.110 g, 50%. ^1H NMR (400 MHz, CDCl_3): δ (ppm) 1.41 (t, $J(\text{PH}) = 3.6$ Hz, 36H, PMe_3), 1.48 (d, $J(\text{PH}) = 7.6$ Hz, 18H, PMe_3), 6.79–6.82 (m, 2H, ant-CH=), 7.58 (s, 2H), 7.58 (d, $J(\text{HH}) = 8.8$ Hz, 2H), 7.82 (d, $J(\text{HH}) = 8.4$ Hz, 2H), 8.17 (s, 2H), 8.28–8.34 (m, 2H, Ru-CH=). ^{13}C NMR (100 MHz, CDCl_3): δ (ppm) 16.62 (t, $J = 15.3$ Hz, PMe_3), 20.09 (d, $J = 21.0$ Hz, PMe_3), 121.40, 123.48, 124.81, 127.58, 130.79, 131.95, 135.23, 137.26 (ant-CH=), 167.30 (Ru-CH=), 202.43 (CO). ^{31}P NMR (160 MHz, CDCl_3): δ (ppm) –21.12 (t, $J = 21.12$ Hz, PMe_3), –9.57 (d, $J = 22.72$ Hz, PMe_3). Anal. Calcd for $\text{C}_{38}\text{H}_{66}\text{Cl}_2\text{O}_2\text{P}_6\text{Ru}_2$: C, 45.02; H, 6.56. Found: C, 44.89; H, 6.81.

$[\{\text{Ru}(\text{PMe}_3)_2(\text{CO})\text{Cl}\}_2(\mu\text{-CH}=\text{CH-ant-CH}=\text{CH-1,8})]$ (**1d**). Yield: 0.048 g, 21%. ^1H NMR (400 MHz, CDCl_3): δ (ppm) 1.44 (t, $J(\text{PH}) = 3.6$ Hz, 36H, PMe_3), 1.49 (d, $J(\text{PH}) = 8.8$ Hz, 18H, PMe_3), 7.39 (t, $J(\text{HH}) = 7.6$ Hz, 2H), 7.56–7.60 (m, 2H, ant-CH=), 7.61 (d, $J(\text{HH}) = 7.2$ Hz, 2H), 7.74 (d, $J(\text{HH}) = 8$ Hz, 2H), 8.35 (s, 1H), 8.44–8.50 (m, 2H, Ru-CH=), 9.40 (s, 1H). ^{13}C NMR (100 MHz, CDCl_3): δ (ppm) 16.92 (t, $J = 15.4$ Hz, PMe_3), 20.15 (d, $J = 20.8$ Hz, PMe_3), 120.61, 124.44, 125.48, 127.92, 128.79, 130.87, 131.81, 133.68, 139.23 (ant-CH=), 171.46 (Ru-CH=), 201.93 (CO). ^{31}P NMR (160 MHz, CDCl_3): δ (ppm) –19.81 (t, $J = 22.56$ Hz, PMe_3), –8.05 (d, $J = 22.56$ Hz, PMe_3). Anal. Calcd for $\text{C}_{38}\text{H}_{66}\text{Cl}_2\text{O}_2\text{P}_6\text{Ru}_2$: C, 45.02; H, 6.56. Found: C, 44.79; H, 6.61.

Crystallographic Details. Single crystals of complexes **1a,c** suitable for X-ray analysis were obtained by slow diffusion of hexane into a solution of dichloromethane and chloroform, respectively. Crystals with approximate dimensions of $0.16 \times 0.12 \times 0.10 \text{ mm}^3$ for **1a** and $0.16 \times 0.12 \times 0.10 \text{ mm}^3$ for **1c** were mounted on glass fibers for diffraction experiments. Intensity data were collected on a Nonius Kappa CCD diffractometer with Mo $K\alpha$ radiation (0.710 73 Å) at room temperature. The structures were solved by a combination of direct methods (SHELXS-97)²³ and Fourier difference techniques and refined by full-matrix least squares (SHELXL-97).²⁴ All non-H atoms were refined anisotropically. The hydrogen atoms were placed in ideal positions and refined as riding atoms. Further crystal data and details of the data collection are summarized in Table 1. Selected bond distances and angles are given in Tables 2 and 3, respectively.

Physical Measurements. ^1H , ^{13}C , and ^{31}P NMR spectra were collected on a Varian Mercury Plus 400 spectrometer (400 MHz) or on a Varian Mercury Plus 600 spectrometer (600 MHz). ^1H and ^{13}C NMR chemical shifts are relative to TMS, and ^{31}P NMR chemical shifts are relative to 85% H_3PO_4 . Elemental analyses (C, H, N) were performed with a Vario ELIII Chnso instrument. UV–vis spectra were recorded on a PDA spectrophotometer by quartz cells with a path length of 1.0 cm. Fluorescence spectra were taken on a Fluoromax-P luminescence spectrometer (Horiba Jobin Yvon Inc.). The electrochemical measurements were performed on a CHI 660C potentiostat (CHI USA). A three-electrode one-compartment cell was used to contain the solution of complexes and supporting electrolyte in dry CH_2Cl_2 . Deaeration of the solution was achieved by argon bubbling through the solution for about 10 min before measurement. The ligand and electrolyte (*n*-Bu₄NPF₆) concentrations were typically 0.001 and 0.1 mol dm^{-3} , respectively. A 500 μm diameter platinum-disk working electrode, a platinum-wire counter electrode, and an Ag/Ag⁺ reference electrode were used. The Ag/Ag⁺ reference electrode contained an internal

solution of 0.01 mol dm⁻³ AgNO₃ in acetonitrile and was incorporated into the cell with a salt bridge containing 0.1 mol dm⁻³ *n*-Bu₄NPF₆ in CH₂Cl₂. All electrochemical experiments were carried out under ambient conditions.

■ ASSOCIATED CONTENT

S Supporting Information. CIF files giving X-ray crystallographic data for [$\{\text{Ru}(\text{PMe}_3)_2(\text{CO})\text{Cl}\}_2(\mu\text{-CH}=\text{CH-ant-CH}=\text{CH-9,10})$] (**1a**) and [$\{\text{Ru}(\text{PMe}_3)_2(\text{CO})\text{Cl}\}_2(\mu\text{-CH}=\text{CH-ant-CH}=\text{CH-2,6})$] (**1c**). This material is available free of charge via the Internet at <http://pubs.acs.org>.

■ AUTHOR INFORMATION

Corresponding Author

*E-mail: chshliu@mail.ccnu.edu.cn (S.H.L.); yinj@mail.ccnu.edu.cn (J.Y.).

■ ACKNOWLEDGMENT

We acknowledge financial support from the National Natural Science Foundation of China (Nos. 20931006, 21072070, 2107-2071, and 20803027) and the Program for Changjiang Scholars and Innovative Research Team in University (No. IRT0953).

■ REFERENCES

- (1) (a) Chen, J.; Reed, M. A.; Rawlett, A. M.; Tour, J. M. *Science* **1999**, *286*, 1550–1552. (b) Feldman, A. K.; Steigerwald, M. L.; Guo, X.; Nuckolls, C. *Acc. Chem. Res.* **2008**, *41*, 1731–1741.
- (2) Ulgut, B.; Abruña, H. D. *Chem. Rev.* **2008**, *108*, 2721–2736.
- (3) (a) Astruc, D. *Acc. Chem. Res.* **1997**, *30*, 383–391. (b) Ceccon, A.; Santi, S.; Orian, L.; Bissello, A. *Coord. Chem. Rev.* **2004**, *248*, 683–724. (c) Carlson, C. N.; Kuehl, C. J.; Da Re, R. E.; Veauthier, J. M.; Schelter, E. J.; Milligan, A. E.; Scott, B. L.; Bauer, E. D.; Thompson, J. D.; Morris, D. E.; John, K. D. *J. Am. Chem. Soc.* **2006**, *128*, 7230–7241. (d) Kaim, W.; Sarkar, B. *Coord. Chem. Rev.* **2007**, *251*, 584–594. (e) Debroy, P.; Roy, S. *Coord. Chem. Rev.* **2007**, *251*, 203–211. (f) Aguirre-Etcheverry, P.; O'Hare, D. *Chem. Rev.* **2010**, *110*, 4839–4864. (g) Gleiter, R.; Werz, D. B. *Chem. Rev.* **2010**, *110*, 4447–4488.
- (4) (a) Balzani, V.; Juris, A.; Venturi, M.; Campagna, S.; Serroni, S. *Chem. Rev.* **1996**, *96*, 759. (b) Delville, M. H. *Inorg. Chim. Acta* **1999**, *291*, 1. (c) Ceccon, A.; Santi, S.; Orian, L.; Bisello, A. *Coord. Chem. Rev.* **2004**, *248*, 683. (d) Adams, H.; Costa, P. J.; Newell, M.; Vickers, S. J.; Ward, M. D.; Felix, V.; Thomas, J. A. *Inorg. Chem.* **2008**, *47*, 11633.
- (5) (a) Horn, C. R.; Martin-Alvarez, J. M.; Gladysz, J. A. *Organometallics* **2002**, *21*, 5386. (b) Bruce, M. I.; Ellis, B. G.; Low, P. J.; Skelton, B. W.; White, A. H. *Organometallics* **2003**, *22*, 3184. (c) Gil-Rubio, J.; Laubender, M.; Werner, H. *Organometallics* **2000**, *19*, 1365. (d) Meyer, W. E.; Amoroso, A. J.; Horn, C. R.; Jaeger, M.; Gladysz, J. A. *Organometallics* **2001**, *20*, 1115. (e) Peters, T. B.; Bohling, J. C.; Arif, A. M.; Gladysz, J. A. *Organometallics* **1999**, *18*, 3261. (f) Sponsler, M. B. *Organometallics* **1995**, *14*, 1920. (g) Dembinski, R.; Bartik, T.; Bartik, B.; Jaeger, M.; Gladysz, J. A. *J. Am. Chem. Soc.* **2000**, *122*, 810. (h) Bruce, M. I.; Low, P. J.; Costuas, K.; Halet, J.-F.; Best, S. P.; Heath, G. A. *J. Am. Chem. Soc.* **2000**, *122*, 1949. (i) Qi, H.; Gupta, A.; Noll, B. C.; Snider, G. L.; Lu, Y.; Lent, C.; Fehlner, T. P. *J. Am. Chem. Soc.* **2005**, *127*, 15218. (j) Xu, G.-L.; Zou, G.; Ni, Y.-H.; DeRosa, M. C.; Crutchley, R. J.; Ren, T. *J. Am. Chem. Soc.* **2003**, *125*, 10057. (k) Xu, G.-L.; Crutchley, R. J.; DeRosa, M. C.; Pan, Q.-J.; Zhang, H.-X.; Wang, X.; Ren, T. *J. Am. Chem. Soc.* **2005**, *127*, 13354. (l) Ying, J.-W.; Liu, I. P.-C.; Xi, B.; Song, Y.; Campana, C.; Zuo, J.-L.; Ren, T. *Angew. Chem., Int. Ed.* **2010**, *49*, 954. (m) Bruce, M. I.; Zaitseva, N. N.; Skelton, B. W.; White, A. H. *J. Organomet. Chem.* **2005**, *690*, 3268. (n) Bruce, M. I.; Kelly, B. D.; Skelton, B. W.; White, A. H. *J. Organomet. Chem.* **2000**, *604*, 150. (o) Coat, F.; Guillemot, M.; Paul, F.; Lapinte, C. *J. Organomet. Chem.* **1999**, *578*, 76. (p) Horn, C. R.; Gladysz, J. A. *J. Eur. Inorg. Chem.* **2003**, 2211. (q) Brady, M.; Weng, W.; Gladysz, J. A. *J. Chem. Soc., Chem. Commun.* **1994**, 2665.
- (6) (a) Chung, M.-C.; Gu, X.; Etzenhouser, B. A.; Spuches, A. M.; Rye, P. T.; Seetharaman, S. K.; Rose, D. J.; Zubietta, J.; Sponsler, M. B. *Organometallics* **2003**, *22*, 3485. (b) Fox, H. H.; Lee, J. K.; Park, L. Y.; Schrock, R. R. *Organometallics* **1993**, *12*, 759. (c) Liu, S. H.; Chen, Y.; Wan, K. L.; Wen, T. B.; Zhou, Z.; Lo, M. F.; Williams, I. D.; Jia, G. *Organometallics* **2002**, *21*, 4984. (d) Gao, L.-B.; Liu, S.-H.; Zhang, L.-Y.; Shi, L.-X.; Chen, Z.-N. *Organometallics* **2006**, *25*, 506. (e) Liu, S. H.; Xia, H.; Wen, T. B.; Zhou, Z. Y.; Jia, G. *Organometallics* **2003**, *22*, 737. (f) Liu, S. H.; Hu, Q. Y.; Xue, P.; Wen, T. B.; Williams, I. D.; Jia, G. *Organometallics* **2005**, *24*, 769. (g) Guillaume, V.; Mahias, V.; Mari, A.; Lapinte, C. *Organometallics* **2000**, *19*, 1422. (h) Xia, H.; Yeung, R. C. Y.; Jia, G. *Organometallics* **1998**, *17*, 4762. (i) Yuan, P.; Wu, X. H.; Yu, G.; Du, D.; Liu, S. H. *J. Organomet. Chem.* **2007**, *692*, 3588.
- (7) (a) Zaumseil, J.; Siringhaus, H. *Chem. Rev.* **2007**, *107*, 1296. (b) Lo, S.-C.; Burn, P. L. *Chem. Rev.* **2007**, *107*, 1097. (c) Anthony, J. E. *Angew. Chem., Int. Ed.* **2008**, *47*, 452.
- (8) (a) Han, J.; Burgess, K. *Chem. Rev.* **2010**, *110*, 2709. (b) Haas, K. L.; Franz, K. J. *Chem. Rev.* **2009**, *109*, 4921.
- (9) (a) de Montigny, F.; Argouarch, G.; Costuas, K.; Halet, J. F.; Roisnel, T.; Toupet, L.; Lapinte, C. *Organometallics* **2005**, *24*, 4558. (b) Vilà, N.; Zhong, Y.-W.; Henderson, J. C.; Abruña, H. D. *Inorg. Chem.* **2010**, *49*, 796. (c) Fabre, M.; Bonvoisin, J. *J. Am. Chem. Soc.* **2007**, *129*, 1434. (d) Cicogna, F.; Gaddi, B.; Ingrosso, G.; Marcaccio, M.; Marchetti, F.; Paolucci, D.; Paolucci, F.; Pinzino, C.; Viglione, R. *Inorg. Chim. Acta* **2004**, *357*, 2915. (e) Bertini, F.; Calucci, L.; Cicogna, F.; Gaddi, B.; Ingrosso, G.; Marcaccio, M.; Marchetti, F.; Paolucci, D.; Paolucci, F.; Pinzino, C. *J. Organomet. Chem.* **2006**, *691*, 2987. (f) Hoshino, Y.; Suzuki, T.; Umeda, H. *Inorg. Chim. Acta* **1996**, *245*, 87. (g) Sharmin, A.; Minazzo, A.; Salassa, L.; Rosenberg, E.; Alexander Ross, J. B.; Kabir, S. E.; Hardcastle, K. I. *Inorg. Chim. Acta* **2008**, *361*, 1624. (h) Gao, L.-B.; Zhang, L.-Y.; Shi, L.-X.; Chen, Z.-N. *Organometallics* **2005**, *24*, 1678. (i) Carano, M.; Careri, M.; Cicogna, F.; D'Ambra, L.; Houben, J. L.; Ingrosso, G.; Marcaccio, M.; Paolucci, F.; Pinzino, C.; Roffia, S. *Organometallics* **2001**, *20*, 3478.
- (10) Nguyen, M.-H.; Yip, J. H. K. *Organometallics* **2010**, *29*, 2422.
- (11) Li, F.; Chen, J.; Chai, X.; Jin, S.; Wu, X.; Yu, G.-A.; Liu, S. H.; Chen, G. Z. *Organometallics* **2011**, *30*, 1830.
- (12) Wu, X. H.; Jin, S.; Liang, J. H.; Li, Z. Y.; Yu, G. A.; Liu, S. H. *Organometallics* **2009**, *28*, 2450.
- (13) Ahmad, N.; Levison, J. J.; Robinson, S. D.; Uttley, M. F.; Wonchoba, E. R.; Parshall, G. W. *Inorg. Synth.* **1974**, *15*, 45.
- (14) Kendall, J. K.; Shechter, H. J. *Org. Chem.* **2001**, *66*, 6643.
- (15) Stone, M. T.; Anderson, H. L. *Chem. Commun.* **2007**, 2387.
- (16) Shao, M.; Chen, G.; Zhao, Y. M. *Synlett* **2008**, 371.
- (17) Goichi, M.; Segawa, K.; Suzuki, S.; Toyota, S. *Synthesis* **2005**, *13*, 2116.
- (18) Nierth, A.; Kobitski, A. Yu.; Nienhaus, G. U.; Jäschke, A. *J. Am. Chem. Soc.* **2010**, *132*, 2646.
- (19) Gouloumis, A.; Gonzalez-Rodriguez, D.; Vázquez, P.; Torres, T.; Liu, S. G.; Echegoyen, L.; Ramey, J.; Hug, G. L.; Guldi, D. M. *J. Am. Chem. Soc.* **2006**, *128*, 12674.
- (20) Ma, H.; Kang, M. S.; Xu, K. S.; Jen, A. K. Y. *Chem. Mater.* **2005**, *17*, 2896.
- (21) Chmiel, J.; Neumann, B.; Stammer, H.-G.; Mittel, N. W. *Chem. Eur. J.* **2010**, *16*, 11906.
- (22) Xia, J.-L.; Zhang, C.; Zhu, X.; Ou, Y.; Jin, G.-J.; Yu, G.-A. *New J. Chem.* **2011**, *35*, 97.
- (23) Sheldrick, G. M. *SHELXS-97, a Program for Crystal Structure Solution*; University of Göttingen: Göttingen, Germany, 1997.
- (24) Sheldrick, G. M. *SHELXL-97, a Program for Crystal Structure Refinement*; University of Göttingen, Göttingen, Germany, 1997.